



ARTICLE

Estimated Ultimate Recovery and Productivity of Deep Shale Gas Horizontal Wells

Haijie Zhang¹, Haifeng Zhao², Ming Jiang^{3,*}, Junwei Pu¹, Yuanping Luo¹, Weiming Chen¹, Tongtong Luo^{1,4}, Zhiqiang Li⁵ and Xinan Yu⁶

¹Exploration and Development Department, Chongqing Shale Gas Exploration and Development Co., Ltd., Chongqing, 401120, China

²Oil & Gas Technology Research Institute, Changqing Oilfield Company, Xi'an, 710018, China

³Exploration and Development Research Institute, Zhejiang Oilfield Company, Hangzhou, 310023, China

⁴Geological Exploration and Development Research Institute, Chuanqing Drilling Engineering Co., Ltd., Chengdu, 610056, China

⁵School of Petroleum and Natural Gas Engineering, Chongqing University of Science and Technology, Chongqing, 401331, China

⁶Technology Department, Chongqing University of Science and Technology, Chongqing, 401331, China

*Corresponding Author: Ming Jiang. Email: jiangm85@petrochina.com.cn

Received: 01 May 2024 Accepted: 13 September 2024 Published: 24 January 2025

ABSTRACT

Pressure control in deep shale gas horizontal wells can reduce the stress sensitivity of hydraulic fractures and improve the estimated ultimate recovery (EUR). In this study, a hydraulic fracture stress sensitivity model is proposed to characterize the effect of pressure drop rate on fracture permeability. Furthermore, a production prediction model is introduced accounting for a non-uniform hydraulic fracture conductivity distribution. The results reveal that increasing the fracture conductivity leads to a rapid daily production increase in the early stages. However, above 0.50 D-cm, a further increase in the fracture conductivity has a limited effect on shale gas production growth. The initial production is lower under pressure-controlled conditions than that under pressure-release. For extended pressure control durations, the cumulative production initially increases and then decreases. For a fracture conductivity of 0.10 D-cm, the increase in production output under controlled-pressure conditions is ~35%. For representative deep shale gas wells (Southern Sichuan, China), if the pressure drop rate under controlled-pressure conditions is reduced from 0.19 to 0.04 MPa/d, the EUR increase for 5 years of pressure-controlled production is 41.0 million, with an increase percentage of ~29%.

KEYWORDS

Deep shale gas; fracture stress sensitivity; pressure-controlled production; production prediction

Nomenclature

F_{CD}	Fracture conductivity considering stress sensitivity, D-cm
K_{fi}	Initial hydraulic fracture permeability, D
W_{fi}	Initial hydraulic fracture width, m
d_f	Stress sensitivity coefficient of shale hydraulic fracture, MPa ⁻¹
$\Delta\sigma_{eff}$	Effective stress variation, MPa



α	Effective stress coefficient, dimensionless
ν	Poisson ratio, dimensionless
γ_f	Pressure sensitivity coefficient of shale hydraulic fracture, MPa^{-1}
Δp	Pore pressure variation, MPa
F_{ARCD}	Average fracture conductivity, D·cm
$F_{CD}(x)$	Conductivity along the hydraulic fracture length, D·cm
L_f	Fracture half-length, m
x	Fracture distance from the borehole, m
K_{ma}	Apparent permeability of the matrix system, D
P_m	Reservoir pressure, MPa
μ_g	Gas viscosity, $\text{mPa}\cdot\text{s}$
ϕ_m	Total matrix porosity, dimensionless
t	The time, days
q_a	Adsorbed gas mass per unit volume of matrix, kg/m^3
ρ_g	Gas density, kg/m^3
q_{mf}	Mass exchange term between the matrix and the fracture, kg/s
Δx	Grid block size along the x direction, m
Δy	Grid block size along the y direction, m
V_b	Matrix grid block volume, m^3
h_f	Reservoir height, m
V_L	Langmuir volume, m^3/kg
P_L	Langmuir pressure, MPa
ρ_s	Shale matrix density, kg/m^3
V_{std}	Gas molar volume under standard conditions, m^3/mol
M_g	Molar molecular mass, kg/mol
P_f	Hydraulic fracture pressure, MPa
ϕ_f	Fracture porosity, dimensionless
q_{well}	Mass flow rate into the wellbore from the artificial fracture, kg/s
W_f	Current hydraulic fracture width, m
K_f	Current hydraulic fracture permeability, D
P_{wf}	Bottom hole flow pressure, MPa
r_{eq}	Equivalent well radius, m
r_w	Well radius, m
V_{bf}	Fracture grid block volume, m^3

1 Introduction

The Sichuan Basin and its surroundings are the hotspots for shale gas in China. At present, shale gas exploration is primarily focused on deep layers, which are expected to become the main source of shale gas production in the future. However, deep shale gas exploration is faced with a series of problems caused by geological conditions, such as high temperatures, pressures, and reservoir stress [1]. In particular, high closure stress often leads to increased fracture stress sensitivity during shale gas production. Moreover, proppants are prone to backflow, embedding, and fracturing, which can significantly reduce fracture permeability [2–4], leading to a rapid decline in shale gas well production and the EUR. To reduce the influence of fracture stress sensitivity on production, various studies have

proposed a pressure control production method for seepage field stress sensitivity alleviation and EUR improvement [5,6]. This method is widely employed in North America, and has been shown to increase single well EUR by about 20%–30% [7,8].

The dynamic behavior of shale gas production is characterized by a rapid decline in the initial output, followed by a transition into a stable production stage. Shale gas production loss under pressure release mainly occurs due to the closure of supported and unsupported fractures [9,10]. Therefore, shale gas production models must consider fracture stress sensitivity to accurately predict production. Certain studies applied exponential functions to characterize the relationship between fracture permeability and pressure [11,12], and initially established a production model considering stress sensitivity [13,14]. However, models employing a constant sensitivity coefficient often fail to reflect the severity of stress sensitivity under different production conditions [15,16]. Yao et al. [17] studied the relationship between principal stress and pore pressure variation and derived a model for pore pressure variation with fracture conductivity in anisotropic shales. They used a variable sensitivity coefficient to characterize fracture stress sensitivity. Mirani et al. [18] established a geomechanical coupling model considering matrix non-Darcy effect, fracture viscoelastic deformation, and natural fracture stress sensitivity, and demonstrated that a low initial production is beneficial to increase the EUR. Jia et al. [19] and Wang et al. [20] proposed a hydraulic fracture stress sensitivity model with a variable sensitivity coefficient, and established a coupling formation fracture dynamic shale gas production model with finite fracture conductivity. They further observed that for this model, the initial production rate under pressure control was lower than that under pressure-release conditions, but the EUR increased significantly. Yang et al. [21] revealed that if the same relation is used to simulate the effect of stress sensitivity on production under different conditions, the production allocation size has little effect on the final EUR. Kumar et al. [22] established a fluid-structure coupling model to simulate shale gas production under complex fracture conditions and optimized the well pressure drop rate using the net present value and bottom-hole pressure drop rate chart. He et al. [23] used embedded discrete fractures to accurately characterize artificial and natural fractures, and studied the effects of fracture and matrix stress sensitivity on shale gas well production. For this model, the production rate increased by 42% under pressure control compared to its absence. Guo et al. [24] proposed an embedded fracture discrete model for shale gas considering creep and stress sensitivity effects, and revealed that only under the former consideration, the production rate was better under pressure-controlled compared to pressure-release conditions. Wu et al. [25] conducted stress sensitivity experiments on shale fractures by using the variable flow pressure method; they showed that the greater the variation in the fracture effective stress, the more obvious the decrease in the artificial fracture permeability.

Numerous studies have established pressure-controlled shale gas production models, recognizing the relationship between fracture stress sensitivity, production pressure difference, and fracture creep [26–28]. Various stress sensitivity coefficients have been used to simulate shale gas production under varying pressure differences [29,30]. These studies have revealed that although the initial output of pressure-controlled production is lower than that of pressure-release production, the EUR eventually reverses and increases over time. Certain studies have also speculated that the cumulative output of pressure-release production is better than that of pressure-controlled production when only stress sensitivity is considered [24,31].

Current pressure-controlled shale gas production models do not fully consider the permeability stress sensitivity of deep shale hydraulic fractures, the non-uniform distribution of hydraulic fracture conductivity, and the influence of unsupported fractures. Moreover, the use of a uniform fracture conductivity and a fixed stress sensitivity coefficient may be inconsistent with practice [19,20,32]. Varying proppant sand concentration and stress sensitivity along the fracture length can lead to the rapid

closure of unsupported or weakly-supported far-end fractures during the production process, effectively reducing the fracture area, and hence, the EUR (Fig. 1).

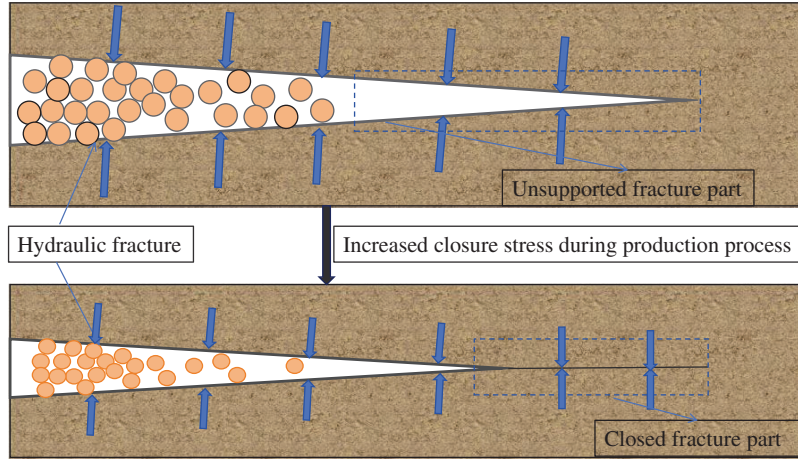


Figure 1: Diagrammatic representation of the rapid closure of unsupported and weakly-supported far-end hydraulic fractures during the shale gas production process

To clarify the internal relationship between pressure-controlled deep shale gas production and the EUR, in this study, we comprehensively considered the effects of stress variation amplitude and the non-uniform distribution of artificial fracture conductivity on the production rate. We assumed the fracture ends to be proppant-free, and used a multi-cluster artificial fracture, characterized by discrete embedded fractures, to establish a pressure-controlled deep shale gas well production prediction model. A simulation study was conducted based on field examples while considering the influence of fracture conductivity, stress sensitivity coefficient, and pressure-controlled production duration on the deep shale gas EUR. The results of this study are of great significance for guiding the development of future pressure-controlled deep shale gas production systems.

2 Hydraulic Fracture Conductivity Model

In the deep shale gas well production process, hydraulic fractures are affected by the increasing effective closure stress. Hydraulic fracture width and propped fracture permeability decrease due to proppant deformation, embedment, and crushing [19]. The attenuation of hydraulic fracture conductivity, F_{CD} , under stress sensitivity consideration, in deep shale can be expressed as [20]

$$F_{CD} = K_{fi} W_{fi} \exp(-d_f \Delta\sigma_{eff}), \quad (1)$$

where $\Delta\sigma_{eff}$ is the change in the effective stress, defined as [33]

$$\Delta\sigma_{eff} = \alpha \frac{(1 - 2\nu)}{(1 - \nu)} \Delta p. \quad (2)$$

By substituting Eqs. (2) in (1), we obtain

$$F_{CD} = K_{fi} W_{fi} \exp(-\gamma_f \Delta p), \quad (3)$$

where γ_f is the shale hydraulic fracture pressure sensitivity coefficient, defined as

$$\gamma_f = \frac{d_f \alpha (1 - 2\nu)}{(1 - \nu)}. \quad (4)$$

Experimental studies have shown the stress sensitivity coefficient to be a variable quantity in the production process. Wu et al. [25] varied the effective stress in the range of 10–40 MPa and observed that the greater the change in effective stress, the more pronounced the fracture permeability stress sensitivity. Therefore, the fracture stress sensitivity coefficient can be considered as a function of the stress change amplitude and stress variation rate during production. In other words, the greater the change in effective stress within a given production period, the higher the fracture stress sensitivity; this relationship can be expressed as

$$d_f = a\Delta\sigma_{eff} + b, \quad (5)$$

where the parameters $a = 0.002 \text{ MPa}^{-2}$ and $b = 0.01 \text{ MPa}^{-1}$ were obtained from experiments.

As the hydraulic fracture width decreases along the fracture length, the influence of the interference between fractures, non-plane propagation of fractures, and non-uniform stress results in the non-uniform distribution of fracture conductivity. Assuming that the average value of the entire fracture is equal, the fracture conductivity can be assumed to be a parabolic distribution, expressed as [32]

$$F_{CD}(x) = \frac{-3F_{ARCD}}{2L_f^2}x^2 + \frac{3}{2}F_{ARCD}. \quad (6)$$

3 Mathematical Model of Matrix-Fracture Coupling Seepage

3.1 Matrix-Seepage

The gas mass conservation equation for the shale gas matrix system while considering the combined effects of microscale effects, such as deep shale gas adsorption/desorption, matrix pore gas slip flow, and surface diffusion can be expressed as [34]

$$\Delta x \frac{\partial}{\partial x} \left(\frac{\Delta y h_f K_{ma} \rho_g}{\mu_g} \frac{\partial P_m}{\partial x} \right) + \Delta y \frac{\partial}{\partial y} \left(\frac{\Delta x h_f K_{ma} \rho_g}{\mu_g} \frac{\partial P_m}{\partial y} \right) - q_{mf} = V_b \frac{\partial(\varphi_m \rho_g)}{\partial t} + V_b \frac{\partial q_a}{\partial t}. \quad (7)$$

Assuming that the gas in the matrix is adsorbed onto the pore wall in the form of a monolayer, we can use the Langmuir isotherm adsorption equation to describe its absolute amount as [34]

$$q_a = \frac{\rho_s M_g}{V_{std}} \frac{V_L P_m}{P_L + P_m}. \quad (8)$$

3.2 Gas Seepage Through Hydraulic Fractures

Taking into account the deformation stress sensitivity and fracture permeability, K_f , the gas seepage equations for the hydraulic fractures can be developed as [13–14,34]

$$\Delta x \frac{\partial}{\partial x} \left(\frac{K_f W_f h_f \rho_g}{\mu_g} \frac{\partial P_f}{\partial x} \right) + q_{mf} - q_{well} = V_{bf} \frac{\partial(\varphi_f \rho_g)}{\partial t}, \quad (9)$$

where q_{well} is the mass flow rate into the wellbore from the artificial fracture, which can be defined for a horizontal well model as

$$q_{well} = \frac{2\pi \rho_g K_f W_f}{\mu_g} \frac{P_f - P_{wf}}{\ln(r_{eq}/r_w)}. \quad (10)$$

We assume the outer boundary of the model to be closed and the inner boundary to be under constant flow pressure, i.e., constant production. Eqs. (1)–(10) constitute the mathematical seepage model for deep

shale gas production prediction. Given an initial fracture permeability and fracture width, the initial fracture conductivity was calculated using Eq. (3), while the conductivity distribution along the fracture length was calculated using Eq. (6). The reservoir and hydraulic fracture systems were meshed and provided with the property parameters, and the pressure distribution of hydraulic fracture and matrix system was obtained by coupling and iteratively solving for the hydraulic fracture seepage (Eq. (9)) and matrix system (Eq. (8)). The apparent permeability of the matrix was updated according to the matrix pressure distribution and the fracture permeability was updated according to the hydraulic fracture grid pressure distribution. Finally, Eq. (10) was used to calculate the production at each time step to obtain the deep shale gas production curve for the preset period.

4 Sensitivity Analysis for Pressure-Controlled Production

We predicted the managed pressure production according to the reservoir and fracture parameters of a shale gas well in Southern Sichuan, China [35]. The horizontal section of the shale gas well is ~2700 m, buried at a depth of 4200 m. The horizontal well has a fracturing length of 2400 m, with a total of 30 fracturing sections and 8 clusters per section. Some sections of the horizontal well are naturally developed fractures. Currently, the exploration of this horizontal well is relatively stable, with a good pressure-controlled production effect (well parameters shown in Table 1).

Table 1: Reservoir and fracturing parameters of a deep shale gas well in eastern Sichuan

Parameter	Value	Unit	Parameter	Value	Unit
Number of fracturing segments	30	–	Number of cluster per section	8	–
Horizontal segment length	2400	m	Cluster spacing	10	m
Well radius	0.1	m	Sensitivity coefficient of stress	0.04	MPa ⁻¹
Flow pressure at the bottom of the well	3	MPa	Initial fracture conductivity	0.1	D·cm
Initial pressure	70	MPa	The fracture length	120	m
Reservoir temperature	139	°C	Fracture height	12	m
Gas saturation	75	%	Gas content	6	m ³ /t
The total matrix porosity	5.2	%	Matrix permeability	100	nD

4.1 Influence of Fracture Conductivity on the EUR

We studied the impact of fracture conductivity on the deep shale gas production in the study area (Fig. 2). As the fracture conductivity increased from 0.01–1.00 D·cm, the cumulative production increased by 100%, indicating a significant effect (Table 2). When the fracture conductivity was increased from 0.01–0.20 D·cm, the cumulative production increased by 108% over three years. Although the percentage of increase decreased over time, it still reached up to 70%. At 0.50 D·cm, the cumulative production increased by 14% in three years. Albeit with a relatively small magnitude, the production rate continued to increase (a cumulative increase of 10% over 20 years). For 1 D·cm, the cumulative production increased by ~10 million m³, while the EUR increased by ~5%. Overall, when the fracture conductivity was increased from 0.01 to 1.00 D·cm, the cumulative production in 20 years increased by a total of 99.32 million m³. However, for a value of 0.50 D·cm, fracture conductivity had a limited effect on shale gas production. The impact of fracture conductivity on production indicates that deep shale gas fractures are sensitive to high stress and fracture conductivity. Therefore, high sand concentration is of great significance for improving the EUR of deep shale gas.

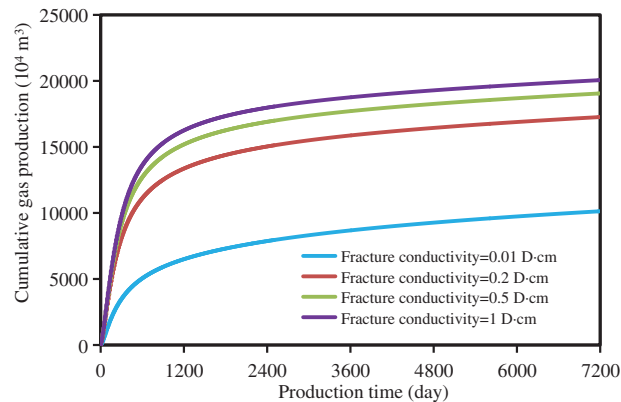


Figure 2: Influence of fracture conductivity on shale gas production and EUR

Table 2: Influence of fracture conductivity on the shale gas production increase percentage

Fracture conductivity (D·cm)	Production increase percentage (3 years)	Production increase percentage (10 years)	Production increase percentage (20 years)
0.01	0	0	0
0.2	108%	83%	70%
0.5	14%	12%	10%
1	7%	6%	5%

4.2 Influence of Pressure-Controlled Production Time on the EUR

According to the predictions for a hydraulic fracture with a fracture conductivity of 0.10 D·cm (Fig. 3a), the production in the initial stages of pressure-release production was significantly higher than that of pressure-controlled production, resulting in a higher cumulative production for the former condition over a certain period. However, as the duration under pressure control increased, the production rate reversed. One year of pressure control had the greatest impact on production growth, with a cumulative production growth rate of 24% over 10 years and 22% over 20 years (Fig. 3b; Table 3). The increase in cumulative production decreased significantly after two years of pressure control compared to one. Cumulative production increased by 8% in 10 years and 7% in 20 years. The increase in cumulative production after 3 years of pressure control was smaller than that after 2 years, with a growth rate of only 3% over both 10 and 20 years. Therefore, controlling pressure for more than a year had little effect on the increase in production, and with the increasing duration, the daily production in the early stages decreased, but the cumulative production in the later stages gradually increased. When pressure control was applied for 3 years, the cumulative production increased by ~44.00 million m³ over 20 years, indicating that pressure-controlled production can significantly improve the EUR of deep shale gas wells.

4.3 Effect of Stress Sensitivity on the EUR

We further analyzed the effect of the stress sensitivity coefficient on the cumulative production of shale gas (Fig. 4). As the stress sensitivity coefficient increased, the cumulative production sharply decreased within a given production time. As the value of the coefficient increased from 0.050 to 0.075 MPa⁻¹, the cumulative production growth rate decreased by 21% over 10 years and by 20% over 20 years. When the coefficient value was further increased to 0.100 MPa⁻¹, the cumulative production decreased by 25% and 24% over 10 and 20 years, respectively. For 0.125 MPa⁻¹, the cumulative production decreased by 24%

and 23% over 10 and 20 years, respectively. Therefore, as the stress sensitivity coefficient increased, the cumulative production consistently and gradually decreased. Moreover, as the stress sensitivity coefficient was increased from 0.050 to 0.125 MPa⁻¹, the total cumulative production loss over 20 years was 138.5 million m³, i.e., a reduction of ~53% (Table 4). These results indicate that hydraulic fracture stress sensitivity is an extremely important factor in deep shale gas extraction, and reducing it is necessary to improve the final EUR.

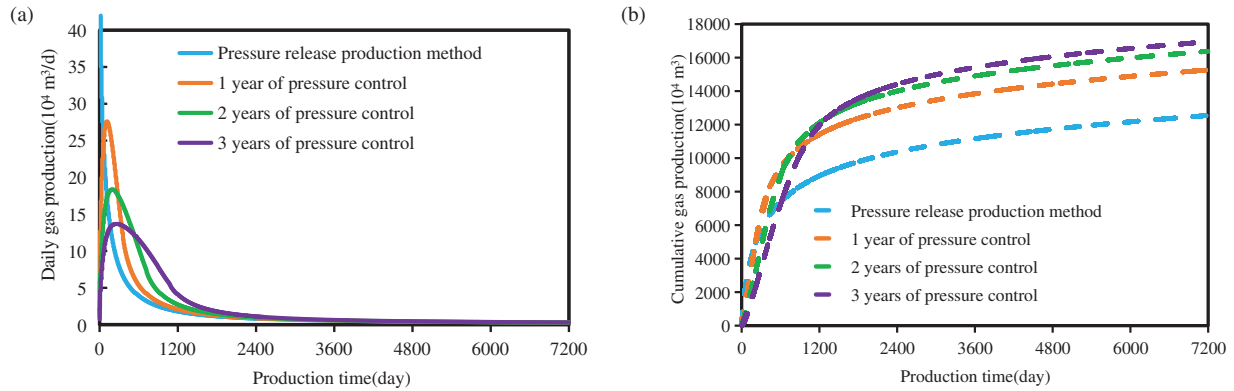


Figure 3: (a) Daily gas production under pressure-controlled and pressure-release conditions. (b) Cumulative production under pressure-controlled and pressure-release conditions

Table 3: Influence of pressure control and pressure release conditions on the increase of shale gas production for a fracture conductivity of 0.10 D·cm

Pressure control production time	Production increase percentage (10 years)	Production increase percentage (20 years)
None	0	0
Controlled pressure production for 1 year	24%	22%
Controlled pressure production for 2 years	8%	7%
Controlled pressure production for 3 years	3%	3%

5 Practical Application of Pressure-Controlled Production

Field monitoring revealed that the horizontal well in the study area has been operational for six months, and its bottom hole pressure has decreased from 75 to ~40 MPa, with an actual pressure drop rate of ~0.19 MPa/d. We assumed the bottom-hole flow pressure to change linearly (Table 5). The influence of different pressure-controlled durations on the production and EUR of the deep shale was examined and the cumulative production rates were obtained (Table 6).

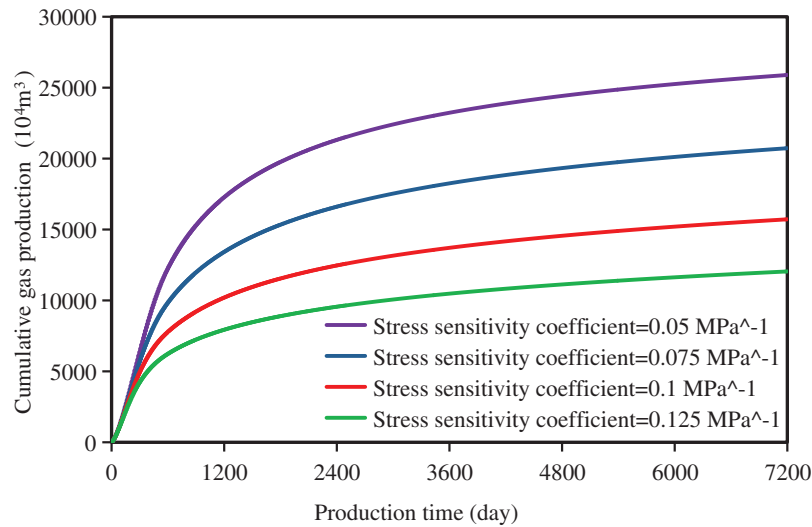


Figure 4: Effect of stress sensitivity coefficient on shale gas well production and EUR

Table 4: Influence of stress sensitivity coefficient on the increase of shale gas production

Stress sensitivity coefficient	Production increase percentage (10 years)	Production increase percentage (20 years)
0.05 MPa ⁻¹	0%	0%
0.075 MPa ⁻¹	-21%	-20%
0.1 MPa ⁻¹	-25%	-24%
0.125 MPa ⁻¹	-24%	-23%

Table 5: Simulation schemes for pressure-controlled deep shale gas well production

Control pressure time	3 months	0.5 year	1 year	3 years	5 years
Pressure drop rate (MPa/d)	0.7	0.35	0.192	0.065	0.039

Table 6: Accumulated production of different pressure control production schemes

Control pressure time	0	3 months	0.5 year	1 year	3 years	5 years
Cumulative gas production for 5 years (10 ⁴ m ³)	8261	9096	9791	10,755	12,824	13,332
Cumulative gas production for 10 years (10 ⁴ m ³)	10,249	11,109	11,829	12,852	15,269	16,417
Cumulative gas production for 20 years (10 ⁴ m ³)	12,177	13,048	13,781	14,831	17,392	18,752

As the pressure-control duration increased, the cumulative shale gas production gradually increased (Fig. 5; Table 6). Increasing the pressure drop rate above the actual rate, i.e., pressure control for 3 months, resulted in a cumulative output loss of 17.0 million m³ over 20 years, whereas, reducing it, i.e., pressure control for 5 years, increased the EUR by ~23.8 million m³. Controlled pressure for 5 years resulted in a EUR increase of ~41.0 million m³ (~29%) compared to that for 3 months. Therefore, based

on this relationship between pressure-controlled production duration and cumulative production, we recommend an optimal pressure-control duration of 3–5 years to maximize shale gas production.

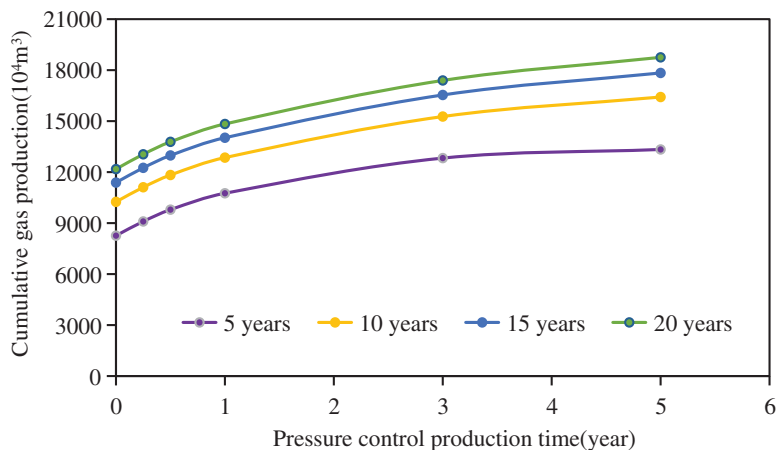


Figure 5: Effect of pressure control durations on shale gas production

6 Conclusion

In this study, we established a deep shale gas production model by considering the hydraulic fracture permeability stress sensitivity and uniform fracture conductivity characteristics. Upon analyzing the influence of pressure-control production duration, fracture conductivity, and stress sensitivity coefficient on the shale gas EUR using this model, we drew the following primary conclusions:

(1) Increasing the initial fracture conductivity increases the daily output along with a gradual increase in the tired production. However, a fracture conductivity value of 0.50 D·cm has a very limited improvement effect on the shale gas production rate.

(2) The initial output of pressure-controlled production is lower than that of pressure-release production. However, with an increase in the pressure control duration, the production rate initially increases and then decreases. Although the early cumulative production is reduced in this case, the output gradually increases over 20 years.

(3) As the stress sensitivity coefficient increases, the cumulative production gradually decreases; for 0.125 MPa⁻¹, the total cumulative production loss of the deep shale gas well over 20 years is predicted to be 138.5 million m³. Therefore, stress sensitivity is a key factor affecting deep shale gas production.

(4) For deep shale gas wells in the study area, increasing the pressure-controlled production duration from 1 to 5 years increases the EUR by 41.0 million (~29%).

Acknowledgement: The authors would like to thank the reviewers and editors for their useful suggestions for the improvement in the quality of our manuscript.

Funding Statement: This work was supported by the Chongqing Natural Science Foundation Innovation and Development Joint Fund (CSTB2023NSCQ-LZX0078) and the Science and Technology Research Program of Chongqing Municipal Education Commission (KJQN202201519), which are gratefully acknowledged.

Author Contributions: The authors confirm contribution to the paper as follows: study conception and design: Haijie Zhang, Zhiqiang Li, Ming Jiang; data collection: Junwei Pu, Tongtong Luo; analysis and interpretation of results: Haifeng Zhao, Xinan Yu, Junwei Pu; draft manuscript preparation: Yuanping

Luo, Weiming Chen; manuscript modifications: Xinan Yu, Ming Jiang. All authors reviewed the results and approved the final version of the manuscript.

Availability of Data and Materials: The data that support the findings of this study are available from the corresponding author upon reasonable request.

Ethics Approval: Not applicable.

Conflicts of Interest: The authors declare no conflicts of interest to report regarding the present study.

References

1. Zhao JZ, Yong R, Hu DF, She CY, Fu YQ, Wu JF, et al. Deep and ultra-deep shale gas fracturing in China: problems, challenges and directions. *Acta Petrolei Sin.* 2024;45(1):295–311.
2. Cao HT, Zhan GW, Zhao Y, Yu XQ. Comparative of conductivity between support fracture and self-support fracture of deep shale reservoir in southern Sichuan basin. *Sci Technol Eng.* 2019;19(33):164–9 (In Chinese).
3. Zhou LL, He SG, Chen C. Measurement of the conductivity of induced fractures in the deep shale in Southern Sichuan basin. *Well Testing.* 2020;29(3):38–44.
4. Liu XW. Influencing factors of hydraulic propped fracture conductivity in shale reservoir. *Fault Block Oil Gas Field.* 2020;27(3):394–8.
5. Okouma V, Guillot F, Sarfare M, Sen V, Ilk D, Blasingame TA. Estimated ultimate recovery (EUR) as a function of production practices in the Haynesville shale. In: *Proceeding of the SPE Annual Technical Conference and Exhibition, 2011 Oct 30–Nov 2; Denver, CO, USA.*
6. Akande J, Spivey JP. Considerations for pore volume stress effects in over-pressured shale gas under controlled drawdown well management strategy. In: *Proceedings of the SPE Canadian Unconventional Resources Conference, 2012 Oct 30–Nov 1; Calgary, AB, Canada.*
7. Wilson K, Hanna ARR. Efficient stress characterization for real-time drawdown management. In: *Proceedings of the Unconventional Resources Technology Conference, 2017 Jul 24–26; Austin, TX, USA.*
8. Wilson K. Analysis of drawdown sensitivity in shale reservoirs using coupled-geomechanics models. In: *Proceedings of the SPE Annual Technical Conference and Exhibition, 2015 Sep 28–30; Houston, TX, USA.*
9. Aybar U, Eshkalak MO, Sepehrmoori K, Patzek TW. The effect of natural fracture's closure on long-term gas production from unconventional resources. *J Nat Gas Sci Eng.* 2014;21:1205–13. doi:10.1016/j.jngse.2014.09.030.
10. Jia P, Ma M, Cao C. Capturing dynamic behavior of propped and unpropped fractures during flowback and early-time production of shale gas wells using a novel flow-geomechanics coupled model. *J Pet Sci Eng.* 2022;208:109412. doi:10.1016/j.petrol.2021.109412.
11. Aybar U, Yu W, Eshkalak MO, Sepehrmoori K, Patzek T. Evaluation of production losses from unconventional shale reservoirs. *J Nat Gas Sci Eng.* 2015;23:509–16. doi:10.1016/j.jngse.2015.02.030.
12. Wang X. Study on the effect of non-uniform conductivity of deep shale gas fracture on productivity (Master's Thesis). China University of Petroleum (Beijing): China; 2019.
13. Li ZQ, Yan WD, Qi ZL, Dong DZ, Huang XL, Yu RZ. Production performance model based on quadruple-porosity medium in shale gas reservoirs considering multi-transport mechanisms. *Energy Source Part A.* 2019;19:1–19. doi:10.1080/15567036.2019.1694103.
14. Jiang M, Li ZQ, Duan GF, Yang JJ, Shi YZ, Shi HQ. Effect of hydraulic fracture conductivity on deep shale gas production. *Xinjiang Oil Gas.* 2023;19(1):35–41 (In Chinese).
15. Huang J, Safari R, Perez O, Fragachan FE. Reservoir depletion-induced proppant embedment and dynamic fracture closure. In: *Proceedings of the SPE Middle East Oil and Gas Show and Conference, 2019 Mar 18–21; Manama, Bahrain.*
16. Pang Y, Soliman MY, Deng H, Hossein E. Analysis of effective porosity and effective permeability in shale-gas reservoirs with consideration of gas adsorption and stress effects. *SPE J.* 2017;22(6):1739–59. doi:10.2118/180260-PA.

17. Yao S, Wang X, Yuan Q, Zeng FH. Transient-rate analysis of stress-sensitive hydraulic fractures: considering the geomechanical effect in anisotropic shale. *SPE Reservoir Eval Eng.* 2018;4:863–88.
18. Mirani A, Marongiu-Porcu M, Wang HY, Enkababian P. Production-pressure-drawdown management for fractured horizontal wells in shale-gas formations. *SPE Reserv Eval Eng.* 2018;21(3):550–65. doi:10.2118/181365-PA.
19. Jia AL, Wei YS, Liu C, Wang JL, Qi YD, Jia CY, et al. A dynamic prediction model of pressure control production performance of shale gas fractured horizontal wells and its application. *Nat Gas Ind B.* 2019;39(6):71–80.
20. Wang J, Luo W, Chen ZA. Integrated approach to optimize bottomhole-pressure-drawdown management for a hydraulically fractured well using a transient inflow performance relationship. *SPE Reserv Eval Eng.* 2020;23(1):95–111. doi:10.2118/195688-PA.
21. Yang B, Luo D, Zhang X, Wu D, Shang SF. A study of stress sensitivity of abnormal high pressure shale gas reservoir and reasonable productivity allocation. *J Southwest Petroleum Univ (Sci Technol Ed).* 2016;38(2):115–21 (In Chinese).
22. Kumar A, Seth P, Shrivastava K, Sharma MM. Optimizing drawdown strategies in wells producing from complex fracture networks. In: *Proceedings of the SPE International Hydraulic Fracturing Technology Conference and Exhibition, 2018 Oct 16–18; Muscat, Oman.*
23. He F, Feng Q, Cui Y. Production schedule optimization of gas wells in W shale gas reservoir under controlled pressure difference based on numerical simulation. *Petroleum Reserv Eval Dev.* 2023;13(1):91–9 (In Chinese).
24. Guo W, Liu JZ, Zhang XW, Teng BL, Kang LX, Gao JL, et al. Study on the mechanism of drawdown management of shale gas horizontal well considering creep effect. *Chin J Theoretical Appl Mech.* 2023;55(3):630–42 (In Chinese).
25. Wu JF, Fan HC, Zhang J, Hu HR, Yuan SS, Li JJ. An experimental study on stress sensitivity of hydraulic fractures in shale: a case study on Longmaxi Formation shale in the southern Sichuan Basin. *Nat Gas Industry.* 2022;42(2):71–81.
26. An C, Killough J, Xia X. Investigating the effects of stress creep and effective stress coefficient on stress-dependent permeability measurements of shale rock. *J Pet Sci Eng.* 2021;198:108155. doi:10.1016/j.petrol.2020.108155.
27. Yu P, Ang L, Li YM, Wu YJ, Xu WJ, Sepehrnoori K. Fractional model for simulating long-term fracture conductivity decay of shale gas and its influences on the well production. *Fuel.* 2023;351:129052. doi:10.1016/j.fuel.2023.129052.
28. Li C, Wang J, Xie H. Anisotropic creep characteristics and mechanism of shale under elevated deviatoric stress. *J Petroleum Sci Eng.* 2020;185:106670. doi:10.1016/j.petrol.2019.106670.
29. Britt LK, Smith MB, Klein HH, Deng JY. Production benefits from complexity-effects of rock fabric, managed drawdown, and propped fracture conductivity. In: *Proceedings of the SPE Hydraulic Fracturing Technology Conference, 2016 Feb 9–11; The Woodlands, TX, USA.*
30. Rojas D, Lerza A. Horizontal well productivity enhancement through drawdown management approach in Vaca Muerta shale. In: *Proceedings of the SPE Canada Unconventional Resources Conference, 2018 Mar 13–14; Calgary, AB, Canada.*
31. Teng BL, Luo WJ, Zhang XW, Liu JZ, Peng Y, Li YH, et al. Study on the mechanism of drawdown management of shale gas reservoir based on creep theory. In: *Proceedings of Chinese Mechanics Conference, 2022; Xi'an, China.*
32. Yang ZZ, Liao ZJ, Li XG, Zhu LY, Chen H. Production simulation of fractured horizontal well with non-uniform space distribution of fracture conductivity in shale gas reservoir. *J Southwest Petroleum Univ (Sci Technol Ed).* 2021;43(3):93–100 (In Chinese).
33. Clarkson CR, Qanbari F, Nobakht M, Heffner L. Incorporating geomechanical and dynamic hydraulic-fracture-property changes into rate-transient analysis: example from the haynesville shale. *SPE Reserv Eval Eng.* 2013;16(3):303–16. doi:10.2118/162526-PA.
34. Li ZQ, Yan WD, Qi ZL, Xiang ZP, Ao X, Huang XL, et al. Prediction of production performance of re-fractured shale gas well considering coupled multi-scale gas flow and geomechanics. *Geofluids.* 2020;2020:9160346.
35. Tang C. Research on productivity prediction model and application to deep shale gas fracturing horizontal wells (Master's Thesis). Chongqing University of Science and Technology: China; 2024.